J|A|C|S
ARTICLES

Published on Web 07/29/2010

Photomagnetic CoFe Prussian Blue Analogues: Role of the Cyanide Ions as Active Electron Transfer Bridges Modulated by Cyanide−Alkali Metal Ion Interactions

Jean-Daniel Cafun,[†] Guillaume Champion,[‡] Marie-Anne Arrio,[§] Christophe Cartier dit Moulin,[‡] and Anne Bleuzen*,[†]

Institut de Chimie Moléculaire et des Matériaux d'Orsay, UMR CNRS 8182, Equipe de Chimie Inorganique, Université Paris-Sud 11, 91405 Orsay Cedex, France, Institut Parisien de Chimie Moléculaire, UMR CNRS 7201, Université Pierre et Marie Curie, Bât. F, 4, place Jussieu, 75252 Paris Cedex 05, France, and Institut de Minéralogie et Physique des Milieux Condensés, UMR CNRS 7590-IPGP, Universités Paris 6 et 7, 4, place Jussieu, 75252 Paris Cedex 05, France

Received March 30, 2010; E-mail: anne.bleuzen@u-psud.fr

Abstract: X-ray absorption spectra at the Co $L_{2,3}$-edges were analyzed by means of ligand field multiplet calculations in different states of three photomagnetic CoFe Prussian blue analogues of chemical formula $Cs_2Co_4[Fe(CN)_6]_{3.3}\cdot 11H_2O$, $Rb_2Co_4[Fe(CN)_6]_{3.3}\cdot 11H_2O$ and $Na_2Co_4[Fe(CN)_6]_{3.3}\cdot 11H_2O$. These simulations of the experimental spectra allowed the quantification of the crystal field parameter (10*Dq*). This determination led us (i) to evidence different behaviors of the Co^{III}(LS) and Co^{II}(HS) ions in the three-dimensional structure related to their electronic configurations, (ii) to propose an approach based on the electronic density distribution along the Co−NC−Fe linkage to account for the energy position of the states implied in the switching properties of the compounds, and (iii) to explain the different photomagnetic properties observed as a function of the size of the inserted alkali cation by competing interactions between the cyanide ion and the transition metal ions within the CoFe cyanide bimetallic network on the one hand and the cyanide ion and the alkali metal ions on the other hand.

Introduction

Recent years have seen the discovery of unusual and fascinating electronic properties in Prussian blue analogues; following the rational elaboration of high magnetic ordering temperature magnets,[1−4] a new generation of compounds exhibiting phenomena involving electronic structure changes in different kind of bimetallic pairs or ions (CoFe,[5−11] MnFe,[12−16] FeCr,[17−19] etc.) mediated by different external stimuli (light,[5,20−22] temperature,[7,23,24] pressure,[19,25−28] etc.) has opened a new

[†] Université Paris-Sud 11.
[‡] Université Pierre et Marie Curie.
[§] Universités Paris 6 et 7.

(1) Gadet, V.; Mallah, T.; Castro, I.; Verdaguer, M.; Veillet, P. *J. Am. Chem. Soc.* **1992**, *114*, 9213–9214.
(2) Mallah, T.; Thiébault, S.; Verdaguer, M.; Veillet, P. *Science* **1993**, *262*, 1554–1557.
(3) Ferlay, S.; Mallah, T.; Ouahès, R.; Veillet, P.; Verdaguer, M. *Nature* **1995**, *378*, 701–702.
(4) Entley, W. R.; Girolami, G. S. *Science* **1995**, *268*, 397–400.
(5) Sato, O.; Iyoda, T.; Fujishima, A.; Hashimoto, K. *Science* **1996**, *272*, 704–705.
(6) Verdaguer, M. *Science* **1996**, *272*, 698–699.
(7) Sato, O.; Einaga, Y.; Fujishima, A.; Hashimoto, K. *Inorg. Chem.* **1999**, *38*, 4405–4412.
(8) Shimamoto, N.; Ohkoshi, S.; Sato, O.; Hashimoto, K. *Inorg. Chem.* **2002**, *41*, 678–684.
(9) Bleuzen, A.; Lomenech, C.; Escax, V.; Villain, F.; Varret, F.; Cartier dit Moulin, C.; Verdaguer, M. *J. Am. Chem. Soc.* **2000**, *122*, 6648–6652.
(10) Cartier dit Moulin, C.; Villain, F.; Bleuzen, A.; Arrio, M.-A.; Sainctavit, P.; Lomenech, C.; Escax, V.; Baudelet, F.; Dartyge, E.; Gallet, J. J.; Verdaguer, M. *J. Am. Chem. Soc.* **2000**, *122*, 6653–6658.
(11) Goujon, A.; Roubeau, O.; Varret, F.; Dolbecq, A.; Bleuzen, A.; Verdaguer, M. *Eur. J. Phys. B* **2000**, *14*, 115–124.
(12) Ohkoshi, S.; Yorozu, S.; Sato, O.; Iyoda, T.; Fujishima, A.; Hashimoto, K. *Appl. Phys. Lett.* **1997**, *10*, 1040–1042.
(13) Tokoro, H.; Matsuda, T.; Hashimoto, K.; Ohkoshi, S. *J. Appl. Phys.* **2005**, *97*, 508–510.
(14) Ohkoshi, S.; Tokoro, H.; Hashimoto, K. *Coord. Chem. Rev.* **2005**, *249*, 1830–1840.
(15) Cobo, S.; Fernandez, R.; Salmon, L.; Molnar, G.; Bousseksou, A. *Eur. J. Inorg. Chem.* **2007**, 1549–1555.
(16) Buschmann, W. E.; Ensling, J.; Gütlich, P.; Miller, J. S. *Chem.−Eur. J.* **1999**, *5*, 3019–3028.
(17) Ohkoshi, S.; Einaga, Y.; Fujishima, A.; Hashimoto, K. *J. Electroanal. Chem.* **1999**, *473*, 245–249.
(18) Ohkoshi, S.; Hashimoto, K. *J. Am. Chem. Soc.* **1999**, *121*, 10591–10597.
(19) Coronado, E.; Jiménez-Lopez, M. C.; Korzeniak, T.; Levchenko, G.; Romero, F. M.; Segura, A.; Garcia-Baonza, V.; Cezar, J. C.; de Groot, F. M. F.; Milner, A.; Paz-Pasternak, M. *J. Am. Chem. Soc.* **2008**, *130*, 15519–15532.
(20) Escax, V.; Bleuzen, A.; Itié, J. P.; Münsch, P.; Varret, F.; Verdaguer, M. *J. Phys. Chem. B* **2003**, *107*, 4763–4767.
(21) Margadonna, S.; Prassides, K.; Fitch, A. N. *Angew. Chem., Int. Ed.* **2004**, *43*, 6316–6319.
(22) Shimamoto, N.; Ohkoshi, S.; Sato, O.; Hashimoto, K. *Chem. Lett.* **2002**, 486–487.
(23) Ohkoshi, S.; Matsuda, T.; Tokoro, H.; Hashimoto, K. *Chem. Mater.* **2005**, *17*, 81–84.
(24) Escax, V.; Bleuzen, A.; Cartier dit Moulin, C.; Villain, F.; Goujon, A.; Varret, F.; Verdaguer, M. *J. Am. Chem. Soc.* **2001**, *123*, 12536–12543.
(25) Moritomo, Y.; Hanawa, M.; Ohishi, Y.; Kato, K.; Takata, M.; Kuriki, A.; Nishibori, E.; Sakata, M.; Ohkoshi, S.; Tokoro, H.; Hashimoto, K. *Phys. Rev. B* **2003**, *68*, 144106.

 10.1021/ja102660b

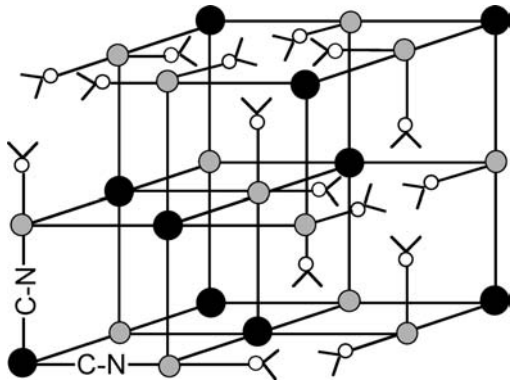

Figure 1. Scheme of the unit cell of the alkali cation free CoFe Prussian blue analogue of chemical formula $Co_4[Fe(CN)_6]_{8/3}\cdot 18H_2O$. Black and gray circles stand for Fe and Co ions, respectively.

research field. Such compounds offer appealing perspective for the elaboration of nanodevices provided the following: (i) the material's working temperature is increased up to room temperature, and (ii) the chemistry is properly tuned to preserve the switching properties at a very small scale. To achieve these goals in a rational way, it is necessary to understand which parameters tune the switching properties in these compounds.

In the well-known face centered cubic structure of the CoFe Prussian blue analogue of chemical formula $C_xCo_4[Fe(CN)_6]_{(8+x)/3}\square_{(4-x)/3}$, $n$$H_2O$, $\square$ represents the intrinsic $[Fe(CN)_6]$ vacancies, which are randomly distributed in the solid. C^+ is an alkali metal ion, and x is the amount of alkali metal ion inserted in a unit cell. The Wyckoff positions 4a (0, 0, 0) are occupied by Fe ions or $\square$, and the 4b positions ($^1/_2$, $^1/_2$, $^1/_2$) are occupied by Co ions.[29] A scheme of the unit cell of the alkali cation free CoFe Prussian blue analogue is shown in Figure 1.

The photomagnetic effect exhibited by CoFe Prussian blue analogues appears only when alkali metal ions are inserted in the structure.[9] The insertion of alkali metal ions is accompanied by a supplementary insertion of $[Fe(CN)_6]$ entities to compensate the charge and therefore by an increase of the NC/OH_2 ligands ratio in the Co coordination sphere.[24]

A first appealing hypothesis was proposed to explain the appearance of the photomagnetic effect and the relative stabilization of the $Co^{III}(LS)Fe^{II}$ and $Co^{II}(HS)Fe^{III}$ states implied in the switching properties. The hypothesis was based on the Co crystal field parameter modulation when the average chemical composition of the Co ion coordination sphere $(Co(NC)_{(8+x)/2}(OH_2)_{(4-x)/2})$ changes.[6,7,9,15,24] In this approach, the progressive insertion of an alkali metal ion would be accompanied by the progressive replacement of weak ligand field water molecules by stronger field N-ligating cyanide ligands in the Co ion coordination sphere, which modulates the potential of the $Co^{III/II}$ redox couple. The Co crystal field parameter would then be a key parameter to tune the relative potential position of the $Co^{III/II}$ and $Fe^{III/II}$ redox couples and therefore the energy position of the $Co^{III}Fe^{II}$ and $Co^{II}Fe^{III}$ states implied in the switching properties of the compounds.

Since a quantitative UV−visible spectroscopic investigation is impossible due to the existence of large charge transfer bands in the visible range (the compounds are all dark purple violet or dark purple brown),[7] X-ray absorption spectra at the transition metal $L_{2,3}$-edges have been simulated by means of ligand field multiplet calculations, which allows the quantification of the crystal field parameter ($10Dq$).[30] The Co^{II} and Co^{III} spectral features, well separated in energy, allow the determination of the crystal field parameter of each ion, even if both are present in the same sample.[31] Using this powerful tool, we showed in short communications that, contrary to expectation, the Co^{II} crystal field parameter in CoFe Prussian blue analogue is weak.[31,32]

In this work, we extend this approach to a series of photomagnetic compounds in which the nature of the alkali metal ion has been varied. The chemical formula of the three photomagnetic compounds under study are the following $Cs_2Co_4[Fe(CN)_6]_{3.3}\cdot 11H_2O$, $Rb_2Co_4[Fe(CN)_6]_{3.3}\cdot 11H_2O$, and $Na_2Co_4[Fe(CN)_6]_{3.3}\cdot 11H_2O$. They are called CsCoFe, RbCoFe, and NaCoFe in the following. The chemical composition of the CoFe bimetallic cyanide network is the same for the three compounds; only the nature of the alkali metal ion varies.[33] The determination of the Co crystal field parameter in this series of compounds leads us to modulate the first proposed explanation for the formation of the switching pairs and the energy position of the states implied in the switching properties of this compounds family. Furthermore, the careful study of the Co $L_{2,3}$-edges spectra in the photoinduced metastable state of compounds containing the same amount of alkali metal ions of different nature shows that interactions between the alkali metal ions and the CoFe cyanide bimetallic network also modulate the energy position of the states implied in the switching properties.

Experimental Section

Synthesis. CsCoFe, RbCoFe, and NaCoFe were synthesized following the experimental conditions used to synthesize the three compounds called Cs_2, $Rb_{1.8}$, and $Na_{1.8}$ in ref 33. Several syntheses were performed until exactly the same stoichiometry for the three compounds was reached. Samples are obtained as powders with particles in the 100−200 nm size range. A typical transmission electron micrograph is shown in the Supporting Information (S14). The elemental analysis and powder X-ray diffraction pattern of the compounds recorded at room temperature and pressure are given in the Supporting Information (S13). CsCoFe, RbCoFe, and NaCoFe strongly resemble Cs_2, $Rb_{1.8}$, and $Na_{1.8}$ in ref 33. Their X-ray diffraction patterns were indexed within the F$m3m$ space group, and the a-cubic lattice parameters calculated from the angle position of the 200, 220, 400, and 420 more intense reflections are 9.98 ± 0.03, 9.96 ± 0.03, and 10.32 ± 0.03 Å for CsCoFe, RbCoFe, and NaCoFe, respectively. The important difference between the lattice parameters of CsCoFe and RbCoFe on the one hand and the lattice parameter of NaCoFe on the other hand reflects the different electronic states of the compounds. At room temperature, NaCoFe is composed of $Co^{II}(HS)$ ions with longer Co to ligand bonds, whereas CsCoFe and RbCoFe are composed of $Co^{III}(LS)$ ions with short Co to ligand bonds. Whatever the oxidation state +II or +III

(26) Ksenofontov, V.; Levchenko, G.; Reiman, S.; Gütlich, P.; Bleuzen, A.; Escax, V.; Verdaguer, M. *Phys. Rev. B* **2003**, *68*, 024415.
(27) Egan, L.; Kamenev, K.; Papanikolaou, D.; Takabayashi, Y.; Margadonna, S. *J. Am. Chem. Soc.* **2006**, *128*, 6034–6035.
(28) Bleuzen, A.; Cafun, J.-D.; Bachschmidt, A.; Verdaguer, M.; Münsch, P.; Baudelet, F.; Itié, J.-P. *J. Phys. Chem. C* **2008**, *112*, 17709–17715.
(29) Lüdi, A.; Güdel, H. U. *Structure and Bonding*; Spinger-Verlag: Berlin, Germany, 1973; pp 1−21; and references herein.
(30) Arrio, M. A.; Sainctavit, P.; Cartier dit Moulin, C.; Mallah, T.; Verdaguer, M.; Pellegrin, E.; Chen, C. T. *J. Am. Chem. Soc.* **1996**, *118*, 6422–6427.
(31) Escax, V.; Champion, G.; Arrio, M.-A.; Zacchigna, M.; Cartier dit Moulin, C.; Bleuzen, A. *Angew. Chem., Int. Ed.* **2005**, *44*, 2–5.
(32) Cartier dit Moulin, C.; Champion, G.; Cafun, J.-D.; Arrio, M.-A.; Bleuzen, A. *Angew. Chem., Int. Ed.* **2007**, *46*, 1–4.
(33) Bleuzen, A.; Escax, V.; Itié, J.-P.; Münsch, P.; Verdaguer, M. *C. R. Chimie* **2003**, *6*, 343–352.

of the Fe ion, the geometry of the $Fe(CN)_6$ entities are very close. The slight difference between the lattice parameters of CsCoFe and RbCoFe lies within the experimental error bar.

X-ray Absorption Spectroscopy (XAS). We recorded the absorption spectra at the cobalt $L_{2,3}$-edges on the BACH beamline (Beamline for Advanced diCHroic experiments) at the ELETTRA synchrotron radiation source (Trieste, Italy).[34] On the BACH beamline, the insertion devices are two APPLE-II undulators.[34] We used the first harmonic of the high-energy undulator. The monochromator is a spherical grating of a groove density of 400 lines/mm giving an intensity of 7×10^{11} photon s^{-1} on the sample at the cobalt L_3-edge energy.

The as-synthesized powdered samples were prepared as homogeneous pellets stuck on the copper head of the sample holder. The experimental end station was the cryostat developed by Kappler and Sainctavit,[35] reaching temperatures ranging from 1.5 to 300 K. The spectra were recorded by measuring the photocurrent emitted by the sample under a vacuum of at least 10^{-9} mbar. The detection was a total yield detection mode. Hence, the measure is surface sensitive (a few tens of angstroms) due to the escape depth of the electrons. The sample had been cooled down to 4 K, and the photomagnetic state was induced by X-ray irradiation. We checked that the transformation was almost saturated in one hour. We also checked that the state induced by X-ray irradiation was the same as the one reached by visible irradiation. The spectra of the compounds "before irradiation" were recorded first. During the acquisition time of the first spectrum, we indeed observed that the phototransformation is quite negligible.

Magnetic Measurements. The DC magnetization was measured with a superconducting quantum interference device (SQUID) magnetometer (Quantum Design MPMS-5) equipped with an optical fiber connected to a laser diode system ($\lambda = 642$ nm, 200 mW·cm^{-2} output power). For the photomagnetic study, the powders were placed between two transparent scotch tapes, whereas high temperature data were taken using gelcaps as sample holders. All the data were taken under an applied magnetic field of 5000 G.

Results

Magnetic and Photomagnetic Properties. The temperature dependence of $\chi_M T$ (T = temperature, χ_M = molar magnetic susceptibility, M = molecular weight) of CsCoFe**,** RbCoFe, and NaCoFe is shown in Figure 2 in heating and cooling mode over the 100−300 K temperature range. The temperature range is limited to the paramagnetic area of interest.

CsCoFe and RbCoFe exhibit a low and constant $\chi_M T$ value. They are indeed mainly composed of $Co^{III}(LS)-Fe^{II}(LS)$ diamagnetic pairs over the whole temperature range.[33]

Contrary to the two other compounds, NaCoFe shows a variable $\chi_M T$ value. Its $\chi_M T$ value significantly decreases from 245 to 230 K on cooling and significantly increases from 265 to 280 K on heating. This temperature behavior of the $\chi_M T$ product is due to a thermally activated electron transfer already reported by Hashimoto and co-workers in a series of CoFe Prussian blue Na derivatives:[8]

$$Co^{III}-NC-Fe^{II} \underset{T\downarrow}{\overset{T\uparrow}{\rightleftharpoons}} Co^{II}-NC-Fe^{III}$$

The $\chi_M T$ value of NaCoFe indicates that the compound is mainly composed of $Co^{II}(HS)Fe^{III}$ pairs at 300 K, while it mainly contains $Co^{III}(LS)$ and Fe^{II} species below 240 K.[36] At low temperature, the three compounds exhibit very close $\chi_M T$ values, and they contain comparable amounts of Co^{III}, Co^{II}, Fe^{III}, and Fe^{II} ions.[33]

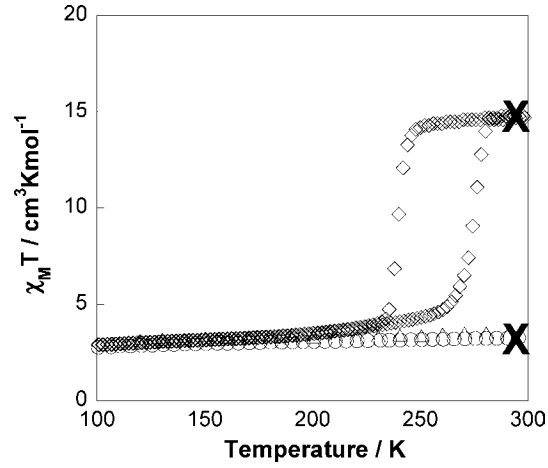

Figure 2. Temperature dependence of the product of the molar magnetic susceptibility and temperature $\chi_M T$ of **CsCoFe** (Δ), **RbCoFe** (○), and **NaCoFe** (◇) in heating and cooling mode over the 100−300 K temperature range. The crosses mark the states that have been studied by XAS.

The temperature dependence of the reduced molar magnetizations (M_M/H) of CsCoFe, RbCoFe, and NaCoFe is shown over the 5−30 K and the 60−160 K temperature ranges before and after irradiation in Figure 3a, c, e and Figure 3b, d, f, respectively.

CsCoFe, RbCoFe, and NaCoFe, all three mainly composed of $Co^{III}(LS)-Fe^{II}(LS)$ diamagnetic pairs at low temperature, exhibit a low magnetization before irradiation. Under irradiation at 10 K, the magnetization of the three compounds increases. They all exhibit a photomagnetic effect. After irradiation, the magnetization of the three compounds remains high and constant. They are all trapped in a photoexcited metastable state with a Curie temperature of 21 K.[9] In exactly the same experimental conditions (same amount of sample, same irradiation conditions, same magnetic measurements conditions), the magnetization increase upon irradiation depends on the nature of the inserted alkali metal ion. The smaller the alkali cation is, the more efficient the photomagnetic effect is. Under the same irradiation conditions, the number of phototransformed CoFe pairs decreases for increasing size of alkali metal ions. Those phototransformed CoFe pairs can either be randomly distributed in the solid or be concentrated in a volume limited by the penetration depth of light, that is, at the surface of the solids. The former case corresponds to various concentrations of phototransformed CoFe pairs within the solids; the latter case corresponds to the same concentration of phototransformed CoFe pairs in various phototransformed volumes of matter. The profile of the temperature dependence of the difference of the magnetization after irradiation and before irradiation ($M_{after} - M_{before}$) is the same for the three compounds over the 5−30 K temperature range (see the Supporting Information S1). The Curie temperature (21 K) is exactly the same in the three compounds. Within the phototransformed volume of the sample, the number of magnetic neighbors is therefore the same, and the amount of phototransformed CoFe pairs also. As for the

(34) Zangrando, M.; Finazzi, M.; Paolucci, G.; Comelli, G.; Diviacco, B.; Walker, R.; Cocco, D.; Parmigiani, F. *Rev. Sci. Instrum.* **2001**, *72*, 1313–1319.

(35) Sainctavit, P. ; Kappler, J.-P. Magnetism and Synchrotron Radiation. In *Lecture Notes in Physics*; Springer: Berlin, Germany, 2001; Vol. 565.

(36) Le Bris, R.; Cafun, J.-D.; Mathonière, C.; Bleuzen, A.; Létard, J.-F. *New J. Chem.* **2009**, *33*, 1255–1261.

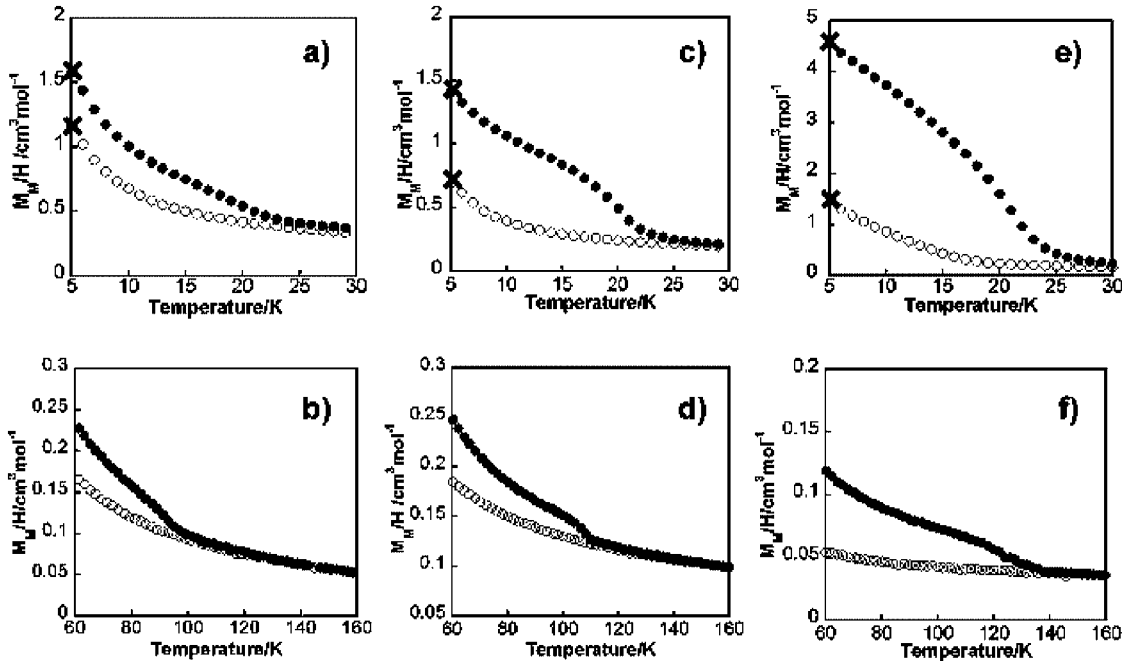

Figure 3. Reduced molar magnetization (M_M/H) as a function of temperature before (○) and after (●) irradiation over the 5−30 K and 60−160 K temperature ranges for CsCoFe (a, b), RbCoFe (c, d), and NaCoFe (e, f). The crosses mark the states that have been studied by XAS.

ground state, the chemical composition and oxidation states of the Co and Fe ions are very close in the metastable excited states of the three compounds; only the nature of the alkali metal ion varies.

The relaxation temperature of the metastable state can be defined as the temperature at which the magnetization before irradiation is recovered. The relaxation temperatures are 95 ± 2, 110 ± 2, and 135 ± 2 K for CsCoFe, RbCoFe, and NaCoFe, respectively. The smaller the alkali cation is, the higher the relaxation temperature is. These experimental results suggest that the alkali cations interact with the bimetallic cyanide network and play a role in the switching properties of the compounds. Because the structure of Prussian blue analogues exhibits a certain degree of disorder due to the presence of various amount of $M(CN)_6$ vacancies, various amount of water molecules and alkali cations and possible slight structural distortion of the M_1-CN-M_2 linkages, some unanswered questions remain on the precise structure of the compounds and particularly on the exact position and role of the alkali cations in the switching properties.

In order to learn more about the CoFe states implied in the switching properties of CoFe Prussian blue analogues, the Co crystal field parameter was determined by X-ray absorption spectroscopy at the Co $L_{2,3}$-edges at 300 K, and at 4 K before and after irradiation. A cross in Figures 2 and 3 marks the studied states.

XAS at the Co $L_{2,3}$-Edges: A Probe of the Co Environment. The XAS spectra at the Co $L_{2,3}$-edges of NaCoFe, RbCoFe, and CsCoFe were recorded at 300 K, and at 4 K before and after irradiation. All the spectra show the same peaks; mostly their intensities vary. The Co $L_{2,3}$-edges spectrum of the rubidium derivative at 4 K before irradiation, representative of all the spectra, is shown in Figure 4. The other spectra are given in the Supporting Information (Figures S2−S4).

Peaks A−D are the signature of Co^{II}(HS) in octahedral symmetry, and peaks E−G, at higher energy, are the signature

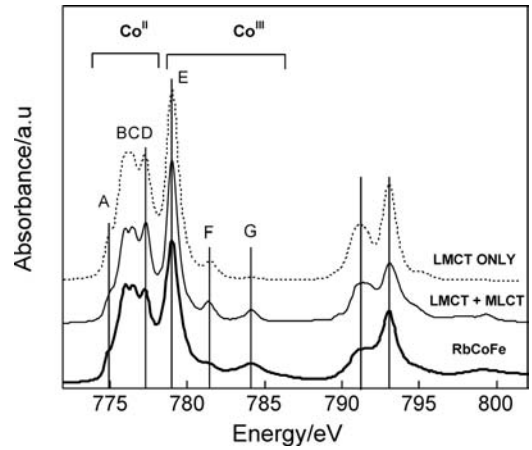

Figure 4. Experimental Co $L_{2,3}$-edges spectrum of RbCoFe recorded at 4 K before irradiation (—) and best simulations obtained from the ligand field multiplet model including LMCT state only (----) and including both MLCT and LMCT states (—).

of Co^{III}(LS) in octahedral symmetry too.[31,32,37,38] The electronic states and the switches from one state to the other observed by XAS are in agreement with the magnetic measurements. In previous work,[31,32,37] we used either the pure ligand field multiplet model to fit the $L_{2,3}$-edges spectra of Co^{II}(HS) ions or the ligand field multiplet model including the ligand to metal charge transfer (LMCT) effects of covalency (Supporting Information S5).[30,39−43] Recently, Bonhommeau et al.[38] used

(37) Cartier dit Moulin, C.; Villain, F.; Bleuzen, A.; Sainctavit, P.; Lomenech, C.; Escax, V.; Baudelet, F.; Dartyge, E.; Gallet, J.-J.; Verdaguer, M. *J. Am. Chem. Soc.* **2000**, *122*, 6653–6658.
(38) Bonhommeau, S.; Pontius, N.; Cobo, S.; Salmon, L.; de Groot, F. M. F.; Molnar, G.; Bousseksou, A.; Dürr, H. A.; Eberhardt, W. *Phys. Chem. Chem. Phys.* **2008**, *10*, 5882–5889.
(39) Thole, B. T.; van der Laan, G.; Fuggle, J. C.; Sawatzky, G.; Karnatak, R. C.; Esteva, J.-M. *Phys. Rev. B* **1985**, *32*, 5107–5118.
(40) Cowan. R. *The Theory of Atomic Structure and Spectra*; University of California Press: Berkeley, California, 1981.

Table 1. Reduction Factor, Crystal Field Parameters, and Charge Transfer Integrals Used to Reproduce the Experimental Co $L_{2,3}$-Edges Spectra of RbCoFe at 4 K before and after Irradiation and the Experimental Co $L_{2,3}$-Edges Spectra of $[Co(H_2O)_6]\cdot(NO_3)_2$ at 300 K[a]

	RbCoFe at 4 K before irradiation		RbCoFe at 4 K after irradiation		$[Co(H_2O)_6]\cdot(NO_3)_2$
	Co^{II}(HS)	Co^{III}(LS)	Co^{II}(HS)	Co^{III}(LS)	Co^{II}(HS)
κ	0.8 (0.68)	0.7 (0.6)	0.8 (0.68)	0.7 (0.6)	0.9 (0.8)
10*Dq* /eV	0.6 (0.7)	2.4 (2.4)	1.1 (1.0)	2.4 (2.4)	1.1 (1.0)
$T(e_g)$ ML	0.5	1.0	0.4	1.0	0.0
$T(t_{2g})$ ML	0.3	0.4	0.2	0.4	0.0
$T(e_g)$ LM	0.9	4.0	1.2	4.0	0.5
$T(t_{2g})$ LM	0.5	3.0	0.8	3.0	0.5

[a] The κ and 10*Dq* values previously determined using the LFM model including the LMCT state only are given in brackets. $T(e_g)$ and $T(t_{2g})$ are the two ligand−metal charge transfer integrals in octahedral symmetry.

the ligand field multiplet model including both LMCT and MLCT states to reproduce the Co $L_{2,3}$-edges spectra of CoFe Prussian blue films. By simultaneously including both LMCT and MLCT states, they showed that the intensity of the peaks associated with the interaction configurations of the calculated spectra are improved and the reduction factor κ, which scales down the Slater−Condon integrals, is closer to the usual experimental reduction in electron repulsion of the free Co ion value.[38] We used therefore the ligand field model including both LMCT and MLCT states to simulate the Co $L_{2,3}$-edges of our compounds (Supporting Information S5). Figure 4 shows the best simulation obtained by using the ligand field multiplet model including the LMCT state only previously used (dotted line) and the ligand field multiplet model including both LMCT and MLCT states (plain line). Figure 4 shows that the use of the ligand field multiplet model including both charge transfers noticeably improves the intensity of peaks F and G on the calculated spectrum as observed by Bonhommeau et al.[38,44] The best simulation of the experimental spectra of NaCoFe, RbCoFe, and CsCoFe at 300 K, 4 K before irradiation, and 4K after irradiation and the parameters used for the calculation are given in the Supporting Information (Figures S2−S4 and Tables S6 and S7).

The Co $L_{2,3}$-edges spectra of NaCoFe, RbCoFe, and CsCoFe at 4 K before irradiation are very close. They were reproduced using the same simulation parameters. The Co $L_{2,3}$-edges spectra of NaCoFe at 300 K, NaCoFe, RbCoFe, and CsCoFe at 4 K after irradiation are also very close. They were therefore, in a first step, also simulated using the same set of simulation parameters. The Co $L_{2,3}$-edges spectrum of the reference compound $[Co^{II}(OH_2)_6](NO_3)_2$ was also simulated using the ligand field multiplet model including both charge transfers. The experimental spectrum, the best simulation, and the parameters used for the calculation are given in the Supporting Information (Figure S8 and Table S9). The values of 10*Dq*, the reduction factor κ, and the charge transfer integrals corresponding to the best simulations are gathered in Table 1, where they are compared to the 10*Dq* and κ values previously determined using the ligand field multiplet model including the LMCT state only.[31,32]

The ligand field multiplet model including both ligand to metal (LMCT) and metal to ligand (MLCT) charge transfers clearly improves the intensity of some peaks and the value of the reduction factor κ, but the values of the simulation parameters remain quite close to the ones obtained by using the ligand field multiplet model including the LMCT state only. The XAS spectra at the Co $L_{2,3}$-edges of CoFe photomagnetic Prussian blue analogues were already rather well-reproduced by the ligand field multiplet model including the ligand to metal charge transfer effects of covalency only probably because the Co ions are surrounded by water molecules and N-ligating cyanide ligands, which are both σ and π donor ligands.[31,33]

Discussion

Co^{III} Crystal Field Parameter. On all the Co $L_{2,3}$-edges spectra, peaks E−G, which are the signature of Co^{III}(LS) species, fall at the same energy position whatever the alkali cation and the populated state, ground or metastable, of the compounds. The Co^{III}(LS) contribution on all the spectra was simulated by using the same set of simulation parameters (Table 1).[31,32] This is at first glance surprising, since the long-range order of the surrounding phase can be very different from one state to the other. Thus, at 4 K before irradiation and at 300 K in the case of the Cs and Rb derivatives, the compounds are mainly composed of Co^{III}(LS) ions. Their cell parameter is short (around 9.96 Å) because Co^{III}(LS) ions to ligand bonds are short (1.96 Å).[10] At 4 K after irradiation and at 300 K in the case of the Na derivative, the cell parameter is significantly longer (around 10.30 Å) because the Co^{II}(HS) ions to ligand bonds are longer (around 2.1 Å)[10] than the Co^{III}(LS) ions to ligand ones. The similarity of the Co^{III}(LS) contributions on all the spectra reflects similar environment of the Co^{III}(LS) species. Despite different long-range structures, the Co^{III}(LS) ions experience almost identical crystal fields, as if the Co^{III}(LS) ions imposed their close environment in the solid. This behavior is probably related to the $(t_{2g})^6(e_g)^0$ electronic configuration of the Co^{III}(LS) ion, for which the octahedral symmetry is highly stabilized and for which strong covalent Co to ligands bonds are expected in agreement with the relatively high value of the $T(e_g)$ and $T(t_{2g})$ LM charge transfer integrals used in the simulations (Table 1).

The 10*Dq*(Co^{III}) value of 2.4 eV is in the expected spectral range for a Co^{III}(LS) ion surrounded by an average of one water molecule and five N-ligating cyanide forming Co^{III}−NC−Fe linear linkages.[45]

Co^{II} Crystal Field Parameter. Contrary to the 10*Dq*(Co^{III}) values, the 10*Dq*(Co^{II}) ones strongly vary from one state to the other.[31,32] This indicates that the Co^{II}(HS) coordination polyhedron is much more flexible than the Co^{III}(LS) one. The Co^{II} crystal field parameters converge toward two values: 0.6 eV for CsCoFe and RbCoFe before irradiation and NaCoFe at 4 K

(41) Butler. P. H. *Point Group Symmetry-Methods and Tables*; Plenum Press:New York, 1991.
(42) de Groot, F. M. F. *Chem. Rev.* **2001**, *101*, 1779–1808.
(43) de Groot, F. M. F. *Coord. Chem. Rev.* **2005**, *249*, 31–63.
(44) The simulation parameters are not the same as those found by Bonhommeau et al. because the spectra of our and their compounds are different. The energy difference between the peaks on our and their spectra is different, which indicates that the environment of the Co ions is not the same. The simulation parameter cannot be directly compared.
(45) Lever, A. *Inorganic Electronic Spectroscopy*, 2nd ed.; Elsevier: Amsterdam, Netherlands, 1984.

before irradiation, and 1.1 eV for CsCoFe, RbCoFe, and NaCoFe at 4 K after irradiation and NaCoFe at 300 K. These two different $10Dq(Co^{II})$ values correspond to different electronic structure of the main Co species of the studied state of the compounds.

The $10Dq(Co^{II})$ value of 0.6 eV corresponds to the states of the compounds essentially composed of Co^{III}(LS) and Fe^{II} ions with the shorter cell parameters (around 9.96 Å) associated with the shorter Co^{III} to ligand distances. This $10Dq$ value is very low and cannot be explained by the chemical composition of the coordination sphere of the Co^{II} ions only. In these states, the coordination polyhedron of the Co^{II}(HS) ions, with significantly longer Co^{II} to ligand bonds than the main Co^{III}(LS) ions ones, is strained and probably distorted from the perfect octahedral geometry. A local structure with bent $Co^{II}-NC-Fe$ linkages accounting for the very low $10Dq(Co^{II})$ value has been proposed in ref 31. These species are not sensitive to light.

The $10Dq(Co^{II})$ value of 1.1 eV corresponds to the states of the compounds essentially composed of Co^{II}(HS) and Fe^{III} ions with the longer cell parameters (around 10.30 Å). This Co^{II} crystal field parameter is the same as the Co^{II} crystal field parameter in the hexaaqua complex determined in exactly the same experimental condition. The N-ligating cyanide ligand in the $Co^{II}-NC-Fe^{III}$ linkages exerts a weak ligand field, comparable to the one exerted by water molecules.[32,45,46] This weak ligand field is related to the π donor character of the N-ligating cyanide ligand in agreement with the relatively high value of the $T(t_{2g})$ LM charge transfer integral used in the simulations (Table 1).

Role of the Cyanide Bridge in the Switching Properties. The occurrence of the switch between both $Co^{III}Fe^{II}$ and $Co^{II}Fe^{III}$ states following an external stimulus is due to the proximity in energy of the $Co^{III}Fe^{II}$ and the $Co^{II}Fe^{III}$ states in the three compounds. The relative stabilization of these states depends on the redox potential of the $Co^{III/II}$ and the $Fe^{III/II}$ couples in their environment. The precursors of CoFe Prussian blue analogues are the $[Co^{II}(OH_2)_6]^{2+}$ and the $[Fe^{III}(CN)_6]^{3-}$ complexes. In the case of the Rb and the Cs derivatives, the $Co^{III}-Fe^{II}$ state is formed at room temperature during the formation of the inorganic polymer, whereas the Co and Fe ions oxidation states in the Na derivative at 300 K are the same as in the precursors. The potentials of the $[Co^{III}(OH_2)_6]^{3+}/[Co^{II}(OH_2)_6]^{2+}$ and the $[Fe^{III}(CN)_6]^{3-}/[Fe^{II}(CN)_6]^{4-}$ redox couples in aqueous solution are reported in Scheme 1.

Given the relative position of the redox potentials, if no reaction occurred between the two precursors, the stable species would remain the $[Co(OH_2)_6]^{2+}$ and $[Fe(CN)_6]^{3-}$ complexes. The redox process leading to the stabilization of the $Co^{III}Fe^{II}$ state is a consequence of the $Co-NC-Fe$ linkages formation, which necessarily induces an increase of the Co ion reducing power. The increase of the reducing power of the Co ion cannot be attributed to an increase of the Co crystal field parameter, since the Co crystal field parameter in the $Co^{II}Fe^{III}$ state of the Na derivative at 300 K, in which the average chemical composition of the Co^{II} coordination sphere is $Co(NC)_5(OH_2)$, is the same as in the $[Co^{II}(OH_2)_6]^{2+}$ complex. Let us consider the formation of $Co-NC-Fe$ linkages. At the carbon side, the C-ligating cyanide is σ donor and π acceptor, and at the nitrogen side, the N-ligating cyanide is σ donor and π donor. In both σ and π systems, the Co to $NC-Fe(CN)_5$ bond formation is expected to be accompanied by an electronic density transfer from the $[Fe(CN)_6]$ entity to the Co ion along the $Co-NC-Fe$ linkage. This electronic density transfer and the negative charge carried by the cyanide bridge are expected to increase the electronic density and then the reducing power of the Co ion. Inversely a slight increase of the redox potential of the $Fe^{III/II}(CN)_6$ couple can be expected. The study of the electrochemical properties of a series of mixed-valence cyano-bridged $Co^{III}Fe^{II}$ dinuclear complexes of chemical formula $[L^nCo^{III}NCFe^{II}(CN)_5]^-$ clearly shows such a modification of the redox properties of the Co and the $[Fe(CN)_6]$ species.[47−52] More precisely, Bernhardt et al. have reported that the replacement of the water molecule by the $-NCFe(CN)_5$ moiety in the $[L^{14}Co^{III}(OH_2)]^{n+}$ complex (L^{14} = 6-methyl-1,4,8,11-tetraazacyclotetradecan-6-amine) shifts the $Co^{III/II}$ redox potential to approximately 400 mV lower potential whereas the presence of the bridged Co units shifts the $Fe^{III/II}$ redox potential of a ferrocyanide solution to approximately 200 mV higher potential.[47] The formation of the $Fe-CN-Co$ linkages during the elaboration of the inorganic polymer modulates the redox potential of the $Fe^{III/II}$ and $Co^{III/II}$ couples, lowering the $Co^{III/II}$ couple with respect to the $Co^{III/II}(OH_2)_6$ one and increasing the $Fe^{III/II}$ couple with respect to the $Fe^{III/II}(CN)_6$ one. In the photomagnetic compounds, the potential of the $Co^{III/II}$ redox couple is lower than the $Fe^{III/II}$ one so that the $Co^{III}-Fe^{II}$ state becomes the ground state. In those compounds, the metastable excited state can be trapped thanks to close energy positions of the $Co^{II}Fe^{III}$ and $Co^{III}Fe^{II}$ states associated with close $Co^{III/II}$ and $Fe^{III/II}$ redox potentials. The cyanide ions play a major role in the switching properties of the compounds as an active electron transfer bridge.

Scheme 1. Redox Potentials of the $Co^{III/II}$ and $Fe^{III/II}$ Couples in the Aqueous Solutions of Precursors, Qualitative Evolution in the Formation of the CoFe Bimetallic Network, and Corresponding Most Stable Species

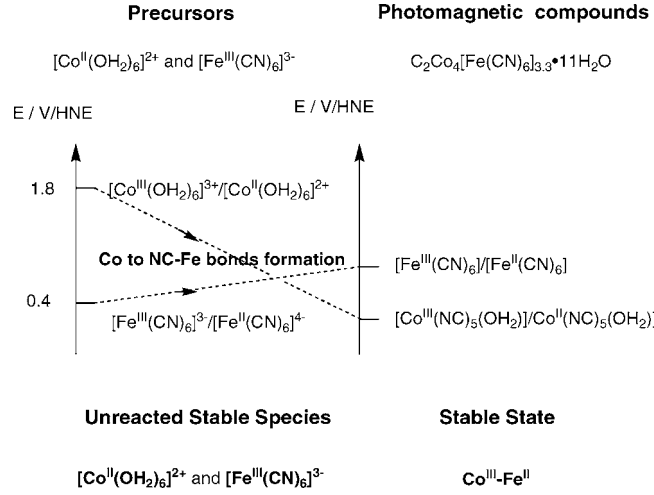

Role of the Alkali Metal Ion in the Photomagnetic Properties. The chemical composition of the $Co_4[Fe(CN)_6]_{3.3}$ cyanide bimetallic network is exactly the same in the three

(46) Johnson, D. A.; Nelson, P. G. *Inorg. Chem.* **1995**, *34*, 5666–5671.
(47) Bernhardt, P. V.; Bozoglian, F.; Brendan, P. M.; Martinez, M.; Gonzalez, G.; Sienra, B. *Eur. J. Inorg. Chem.* **2003**, *13*, 2512–2518.
(48) Bagger, S.; Stoltze, P. *Acta Chem. Scand., Ser. A* **1983**, *37*, 247–250.
(49) Bernhardt, P. V.; Martinez, M. *Inorg. Chem.* **1999**, *38*, 424–425.
(50) Bernhardt, P. V.; Bozoglian, F.; Brendan, P. M.; Martinez, M. *Coord. Chem. Rev.* **2005**, *249*, 1902–1916.
(51) Bernhardt, P. V.; Bozoglian, F.; Brendan, P. M.; Martinez, M.; Merbach, A. E.; Gonzalez, G.; Sienra, B. *Inorg. Chem.* **2004**, *43*, 7187–7195.
(52) Bernhardt, P. V.; Brendan, P. M.; Martinez, M. *Inorg. Chem.* **2000**, *39*, 5203–5208.

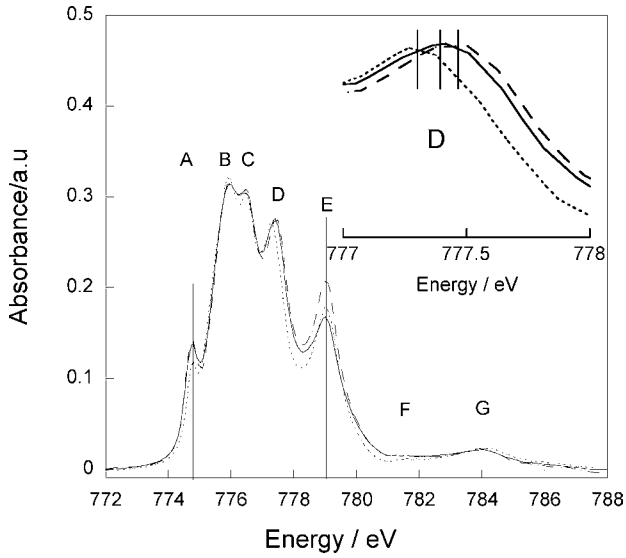

Figure 5. Superimposition of experimental Co L_3-edge spectra of NaCoFe (····), RbCoFe (—), and CsCoFe (----) recorded at 4 K after irradiation. Inset: enlargement of peak D showing that its energy position slightly changes for increasing size of the alkali metal ions.

studied compounds, and yet, the switching properties are different. We can suppose that these differences are linked to different interactions between the alkali metal ion and the cyanide bimetallic network. In order to detect any small change of the electronic structure of the cobalt ions related to theses interactions, the Co L_3-edge spectra were even more carefully examined.

Before Irradiation at 4 K, the three compounds are essentially composed of $Co^{III}(LS)Fe^{II}$ pairs, and the E, F, and G peaks corresponding to the contribution of the $Co^{III}(LS)$ ions are situated at exactly the same energy position (Figure S10 in the Supporting Information). The electronic structure of the $Co^{III}(LS)$ ions is the same within the experimental resolution from one compound to the other. The $Co_4[Fe(CN)_6]_{3.3}$ cyanide bimetallic network is mainly composed of $Co^{III}(LS)-NC-Fe^{II}$ linkages with strong covalent $Fe^{II}-C$, NC, and $Co^{III}-N$ chemical bonds. In this state, the interactions between the transition metal ions and the cyanide ions are much stronger than any weak interaction between the cyanide ions and the alkali cations. The effect of the latter on the former is negligible. Therefore, the electronic structure of the $Co^{III}(LS)$ ions and the $Co^{III}(LS)Fe^{II}$ ground states are the same or very close in the three compounds.

The Co L_3-edge spectra of the three compounds at 4 K **after irradiation** are superimposed in Figure 5. The three spectra are very close to each other and can be reproduced by the same parameters set (see above), but the careful examination of their superimposition makes appear slight differences.

Peaks A, B, and C being located at exactly the same energy position, the energy position of peak D slightly increases for increasing size of the alkali metal ion. Because all the spectra were recorded during the same shift, in exactly the same experimental conditions, the slight difference between the three spectra is significant. Moreover, the shift is observed for peak D only, the other peaks remaining at exactly the same energy. This slight difference cannot be attributed to different relative intensities of the Co^{II} (D peak) and Co^{III} (E peak) ions contributions as shown by linear combinations of various amounts of Co^{II} and Co^{III} ions contributions (see Figure S11 in the Supporting Information). In order to evidence a link between this difference and the photomagnetic properties change, the thermal relaxation temperature of the three compounds was plotted as a function of the energy difference between peaks D and A maxima called E_{AD} in the following (Figure S12 in the Supporting Information). The linear variation evidence a relationship between both experimental observations.

In order to understand the reasons for the differences in the Co L_3-edge spectrum after irradiation along the series of compounds, the effect of a change of the different simulation parameters on the calculated spectrum was investigated. Because the changes in the simulation parameters are small and because several parameters can simultaneously change, the slight differences in the spectra were not quantified. An increase of the κ value or an increase of the $10Dq(Co^{II})$ parameter increases the E_{AD} energy gap but also modifies the energy position of the other peaks (B and C), which is not experimentally observed. In order to maintain constant the energy position of peaks A, B, and C, the κ and the $10Dq(Co^{II})$ values have to be fixed. An increase of the E_{AD} energy gap only is well-reproduced by an increase of both charge transfer integrals values. A higher E_{AD} energy difference is then associated with an increase of the orbital interaction between the cyanide anions and the Co^{II} ions. The relationship between the E_{AD} difference and the thermal relaxation temperature can then be explained. An increase of the E_{AD} difference indicates an increase of the orbital interactions between the cyanide anions and the Co ions, which induces an increase of the reducing power of the Co^{II} ion (enhancement of the Fe to Co electronic density transfer along the $Fe-CN-Co$ linkage). This increase of the reducing power of the Co^{II} ion slightly destabilizes the $Co^{II}(HS)Fe^{III}$ metastable state. A slight destabilization of the $Co^{II}(HS)Fe^{III}$ metastable state decreases the activation energy barrier between the $Co^{II}(HS)Fe^{III}$ metastable state and the $Co^{III}(LS)Fe^{II}$ ground state potential minima, which is indeed expected to decrease the thermal relaxation temperature.

The modulation of the orbital interactions and the switching properties change along the series of compounds can be explained by competing interactions between the cyanide ions and the transition metal ions on the one hand and the cyanide ions and the alkali metal ions on the other hand in the $Co^{II}(HS)Fe^{III}$ metastable state. In the $Co^{II}(HS)Fe^{III}$ state, the Co to cyanide bond is much weaker than in the $Co^{III}(LS)Fe^{II}$ state, so that the interactions between the cyanide anions and the alkali metal ions slightly affect the former. Cesium is the biggest alkali metal ion and the less polarizing; the interactions between this alkali cation and the cyanide anions are expected to be the weakest. In the series of compounds, the orbital interaction between the Co^{II} ions and the cyanide ions are then expected to be the strongest with the highest E_{AD} difference and the lowest relaxation temperature, which is indeed experimentally observed for this Cs derivative. When the size of the alkali cation decreases, it becomes more and more polarizing, and its interactions with the cyanide anions are expected to strengthen. Due to these competing interactions, the orbital interactions between the cyanide anions and the $Co^{II}(HS)$ ions slightly decrease, which is accompanied by a decrease of the E_{AD} difference, a slight stabilization of the $Co^{II}Fe^{III}$ metastable excited state and an increase of the thermal relaxation temperature, which is experimentally observed; the E_{AD} difference decreases from the cesium to the sodium derivative, and the thermal relaxation temperature increases from the cesium to the sodium derivative. Qualitative energy position of the potential

Scheme 2. Qualitative Position of the Redox Potentials of the $Co^{III/II}$ and $Fe^{III/II}$ Couples and Qualitative Energy Position of the $Co^{III}Fe^{II}$ and $Co^{II}Fe^{III}$ States for the Three Compounds

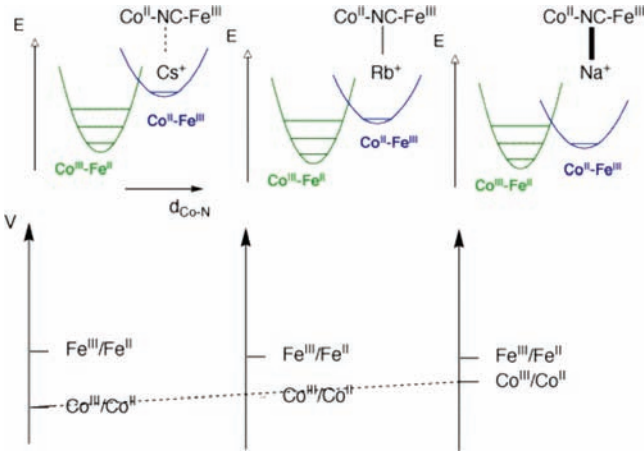

wells corresponding to the ground and the metastable excited states are proposed in Scheme 2 for the three compounds.

In the Na derivative, the orbital interaction between the cyanide anions and the Co^{II}(HS) ions is the weakest. This stabilizes the Co^{II}(HS)Fe^{III} state, which is even populated at room temperature. In the rubidium and cesium derivatives, the energy position of the Co^{II}(HS)Fe^{III} state is higher, which prevents the population of these states at room temperature. It is noticeable that very weak interactions such as interactions between the alkali cations and the cyanide bimetallic network can be responsible for significant change in the switching properties of the compounds: population of different electronic states at 300 K and 95−135 K temperature variation of the thermal relaxation. Such competitive interactions between the cyanide ions and the transition and the alkali metal ions have been recently directly evidenced by Her et al. in MnMn Prussian blue analogues.[53]

Conclusion

XAS spectroscopy turns out to be a fruitful tool that allowed the determination of the Co crystal field parameters in different states of three photomagnetic CoFe Prussian blue analogues. This experimental determination allows us to draw conclusions, which considerably furthers the understanding of those tricky compounds:

(1) The $10Dq(Co^{III}(LS))$ and $10Dq(Co^{II}(HS))$ values reflect different behaviors of both Co^{III}(LS) and Co^{II}(HS) species in the three-dimensional structure. The former, always found in very close environments, forms strong covalent bonds within the cyanide bimetallic network in agreement with its $(t_{2g})^6(e_g)^0$ electronic configuration and the expected high stabilization in octahedral symmetry. The latter, found in various environments, forms weaker bonds within the cyanide bimetallic network in agreement with its $(t_{2g})^5(e_g)^2$ electronic configuration with two electrons in antibonding orbitals.[28]

(2) The determination of the Co crystal field parameter of the main species in the ground and the metastable excited states allows us to show that the Co crystal field parameter is not the driving force in the relative stabilization of the $Co^{III}Fe^{II}$ and $Co^{II}Fe^{III}$ states. We propose another approach based on the electronic density distribution along the Co−NC−Fe linkages and a crucial role of the cyanide bridge acting as an active electron transfer bridge.

(3) The careful examination of the Co $L_{2,3}$-edges shows slight differences in the photoexcited metastable states of the three compounds related to thermal relaxation temperature changes from one compound to the other. This result led us to propose a role of the alkali metal ion in the photomagnetic properties of those compounds. In the ground states of the sample, the covalent bonds forming the cyanide Co^{III}−NC−Fe^{II} bimetallic network are much stronger than any interaction between the alkali metal ions and the cyanide bimetallic network. The Co^{III} ions contribution to the Co $L_{2,3}$-edges are the same in the three compounds. In the photoexcited metastable state, the Co^{II}−N bonds forming the cyanide Co^{II}−NC−Fe^{III} bimetallic network are weaker and the interactions between the alkali metal ions and the cyanide ion compete with the interactions between the Co^{II}(HS) ions and the cyanide ion, which modulates the switching properties.

Acknowledgment. This research was carried out with the support of the CNRS, the University Paris-Sud 11, the University Paris 6, MAGMANet, and the GDR (Magnétisme et Commutation Moléculaire). We thank S. Bonhommeau for providing Co^{II} and Co^{III} ions rcg2, rac2, ban2, and plo2 programming files.

Supporting Information Available: Powder X-ray diffraction pattern and elemental analysis of the compounds (S13), thermal relaxation temperature plotted against E_{AD} (S12), typical transmission electron micrographs of CoFe Prussian blue analogues (S14), ligand field multiplet calculations (S5), all the Co $L_{2,3}$-edges experimental spectra and best simulations (S2−S4, S8), calculation parameters (S6, S7, S9), comparisons or superimpositions of curves mentioned in the main text (S1, S10, S11). This material is available free of charge via the Internet at http://pubs.acs.org.

JA102660B

(53) Her, J.; Stephens, P. W.; Kareis, C. M.; Moore, J. G.; Sik Min, K.; Park, J.; Bali, G.; Kennon, B. S.; Miller, J. S. *Inorg. Chem.* **2010**, *49*, 1524–1534.